LONG-TERM TRENDS AND SPATIOTEMPORAL VARIATIONS OF CLIMATE COMFORT IN CHINA DURING 1966-2016

by

Fei-Fei WU, Xiao-Hua YANG*, Zhen-Yao SHEN, and Ze-Ji YI

State Key Laboratory of Water Environment Simulation, School of Environment, Beijing Normal University, Beijing, China

Original scientific paper
https://doi.org/10.2298/TSCI2004445W

Climate comfort and its variability are of great importance to human comfort, health and well-being, as humans may suffer dire consequences when they are exposed to the environments with heat or cold stress. The climate comfort index represented the integrated effects of meteorological variables on the human thermal sensation. The annual and seasonal climate comfort index values were calculated based on the monthly data of the temperature, relative humidity, and wind speed from 591 stations in China between 1966 and 2016. Using the empirical orthogonal function analysis, the dominant modes of climate comfort index variations were extracted by the first two modes, which accounted for more than 50% of the total variance. The results showed that the annual and seasonal climate comfort index values displayed a latitudinal gradient, and increased towards the south except for the Qinghai-Tibet Plateau. The most frequently perceived thermal sensations were labeled as "cold", "comfortable", "cold" and "extremely cold" conditions from spring to winter, respectively. For annual and seasonal climate comfort index, the consistent increasing trend was detected in most regions of China in the first mode. The sensitive areas were mainly located in the central, eastern and southern China in winter, while in the northern and western China in summer. In the second mode, the fluctuations between upward and downward trends were observed. The sensitive areas were located in the central China in summer, in the southwestern and southern China in autumn, and in the northern China in winter. This study provides the important information for the improvement of human settlement comfort.

Key words: *spatiotemporal variations, climate comfort index, eigenvectors, associated time series, China*

Introduction

Human comfort, health and well-being are influenced by weather conditions [1]. The comfort state of environment is a result of the multifaceted influence of many atmospheric factors, such as the temperature, relative humidity, wind speed, and others [2, 3]. Global warming and significant increase of temperature have greatly changed the thermal comfort and humans' health in different regions [4]. In addition, the relative humidity and wind speed are important to human comfort conditions in the climatic view [5-7]. All of them significantly affect the regional climate, microbial exposures, air quality, and human health [8, 9]. The climate comfort index (CCI) represents the integrated effect on sensation including all relevant variables, which include the temperature, relative humidity, and wind speed.

* Corresponding author, e-mail: xiaohuayang@bnu.edu.cn

A growing number of climate comfort studies have been conducted all over the world. For example, Terjun [10] adopted the comfort index and wind effect index to analyze the physiologic climates of the contentious United States. Xu *et al.* [7] analyzed the differences of the temperature and humidity and the vertical distribution of human comfort in Heilongjiang province in summer. Wang *et al.* [11] evaluated the non-linear relationship between extreme temperature and mortality in different temperature zones in 122 communities across China. However, few studies focused on the long trends and spatiotemporal variations of outdoor thermal comfort in China. China is considered to be one of the world's most vulnerable countries to climate change. In addition, the variability of the climate comfort in China has complex spatial and temporal characteristics on account of the huge differences in the climatic background, climate driving forces and regional characteristics. Therefore, it is necessary to conduct the spatiotemporal analysis of climate comfort at multiple spatial and temporal scales based on the long-time data series.

The objective of this study was to analyze the variability of climate comfort at annual and seasonal scales in China, which will be of great significance for the human settlement improvement. Using the empirical orthogonal function (EOF) analysis, the dominant spatial variations and associated temporal trends of annual and seasonal CCI were extracted [12, 13]. To improve the physical interpretation of these patterns, the spatial patterns were interpolated using the inverse distance weighting (IDW) interpolation method, and the temporal series were analyzed with the 3-year moving average method. This study is not only helpful in the understanding the climate comfort response to global warming but also provides the important information for the improvement of human settlement comfort.

Methods

Algorithm of climate comfort index

The formula of CCI is expressed as:

$$CCI = 1.8t - 0.55(1.8t - 26)\left(1 - \frac{r}{100}\right) - 3.2\sqrt{v} + 32 \tag{1}$$

where climate comfort index is of human settlement, t – the temperature, r – the relative humidity, and v – the wind speed. The CCI values are divided into 9 grades shown in tab. 1.

Table 1. Classification of the CCI values

Grade	CCI range	Sensation	Physiological stress
1	CCI ≤ 25	Extremely cold	Extremely uncomfortable, exposed flesh freezes
2	25 < CCI ≤ 38	Very cold	Very uncomfortable
3	38 < CCI ≤ 50	Cold	Uncomfortable
4	50 < CCI ≤ 55	Cool	Relatively comfortable, slight cold stress
5	55 < CCI ≤ 70	Comfortable	No thermal stress
6	70 < CCI ≤ 75	Warm	Relatively comfortable
7	75 < CCI ≤ 80	Hot	Uncomfortable
8	80 < CCI ≤ 85	Very hot	Very uncomfortable
9	CCI > 85	Torrid	Extremely uncomfortable, exposed heat stroke

Methodology

The aim of EOF analysis is to find a small number of orthogonal base functions as well as associated coefficients to represent the original data [13, 14]. It has been widely used in the climate studies to analyze the dominant modes of variability [15-17]. It decomposes the observed variability into a set of EOF, which are invariant in time, and a set of time series called principal components (PC), which are invariant in space [18-21]. Steps to EOF analysis are:

– Step 1. Calculate the annual and seasonal CCI values at 591 stations based on the monthly data of the temperature, relative humidity and wind speed using eq. (1).
– Step 2. Establish the spatial matrix of annual and seasonal CCI between 1966 and 2016, which contains 51 observations from 591 stations.
– Step 3. Define the normalized matrix X.
– Step 4. Define the spatial covariance matrix C.
– Step 5. Produce eigenvectors (EOF) and time series (PC) associated with EOF by the Eigen-analysis:

$$C \times EOF = V \times EOF \tag{2}$$

where each column in EOF represents eigenvectors of matrix C which describes a spatial pattern, the associated PC describing temporal variations by:

$$PC = EOF^T \times X \tag{3}$$

– Step 6. Analyze the dominant spatial EOF and associated temporal PC. The EOF were interpolated by the IDW interpolation and PC were analyzed by the 3-year moving average method.

Case study

The monthly dataset of the temperature, relative humidity and wind speed in China was provided by the National Climate Center, China Meteorological Administration. The dataset was available for 591 stations with continuous time series between 1966 and 2016, fig. 1.

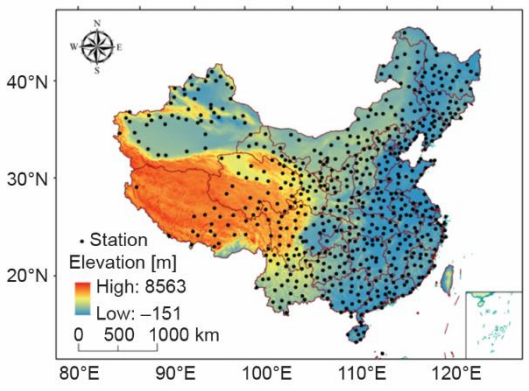

Figure 1. Study area and weather stations in China

The climate comfort has strong temporal, intra-seasonal and inter-seasonal variability. This section first presented the spatial pattern of the climate comfort condition during 1966-2016 at annual and seasonal scales. Next, the spatial and temporal characteristics of climate comfort variations were analyzed using the EOF analysis. The leading EOF and associated PC were used to reflect the spatial and temporal characteristics of climate comfort variations, which extracted most of the variance of original dataset. Table 2 shows the percentage of explained variance of the first ten EOF, which were ranked in a decreasing order. The first and second EOF extracted more than 50% of the total variance, while other EOF series explained

less than 10% of the total variance. Schreck III and Semazzi [22] suggested that the eigenmodes represented noise beyond the second mode. Therefore, the first two EOF series were used to explain the dominant spatiotemporal variations of CCI in this study.

Table 2. Variance contributions of the first ten leading EOF of CCI

	1	2	3	4	5	6	7	8	9	10
Year	60.1	8.0	6.5	3.5	2.5	2.3	1.9	1.6	1.4	1.0
Spring	50.4	12.7	7.6	7.0	2.6	2.4	2.2	1.7	1.1	1.1
Summer	44.7	10.3	7.5	5.5	4.1	2.9	2.6	2.1	1.7	1.5
Autumn	54.3	9.9	5.9	4.3	3.1	2.9	2.2	1.9	1.6	1.4
Winter	47.5	12.4	7.7	5.2	3.1	2.9	2.5	1.8	1.4	1.3

The characteristics of CCI in China during 1966-2016

The spatial distribution of annual and seasonal CCI across China was analyzed using the IDW interpolation method, shown in fig. 2. It was notable that the annual and seasonal CCI values showed a latitudinal gradient, and they generally increased towards the south except for the Qinghai-Tibet Plateau. This phenomenon was consistent with the spatial patterns of Universal Thermal Climate Index [16]. The annual CCI values fluctuated between 24.0 and 70.6, which indicated that the grades of physiological sensation ranged from the extremely cold condition to the warm condition. For annual CCI, the most frequently perceived thermal sensation was the *cold* condition, which accounted for 46.4% of the total area. For seasonal CCI, the most frequently perceived thermal sensations were the *cold*, *comfortable*, *cold* and *extremely cold* conditions from spring to winter, respectively. The large percentage of the *extremely cold* stress (41.7%) and *cold* stress (34.9%) made the cold season the most uncomfortable.

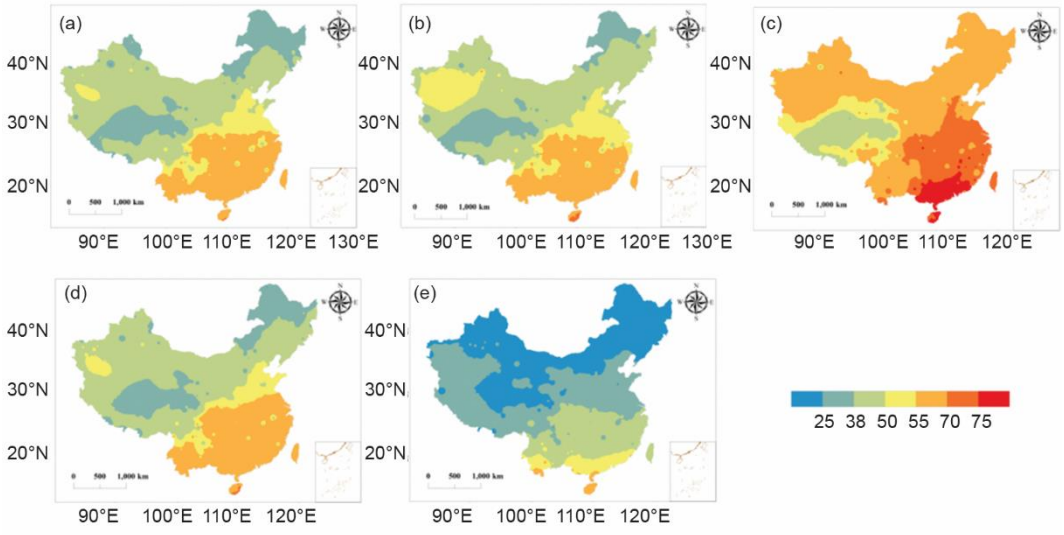

Figure 2. Spatial distribution of annual and seasonal CCI during 1966-2016 in China

As shown in fig. 2(a), four dominant stress levels of annual CCI were identified across China. The uncomfortable areas with the *cold* stress were the largest, which accounted for 46.4% of the total area of China. The regions featured with the *no thermal stress* condition were mainly located in the central, eastern and southern China. It accounted for 20.4% of the total area of China. The climate in these regions was comfortable. Affected by the alpine plateau climate and the high altitude, the sensation in the Tibet Plateau was dominant with the *cold* and *cool* conditions. The climate was very uncomfortable in the northeastern China (*i. e.* Heihongjiang and Jilin Province), as well as the northwestern China (*i. e.* the south of the Tibet Plateau). The spatial distribution of annual CCI was similar to that in spring and autumn, whereas it was distinctly different from that in summer and winter. The CCI values ranged from 37 to over 75 in summer, while it ranged from below 25 to 63 in winter. In the southeastern China, the climate was hot and uncomfortable to people affected by the subtropical and tropical monsoon climates [11]. By contrast, it was comfortable or relatively comfortable in winter.

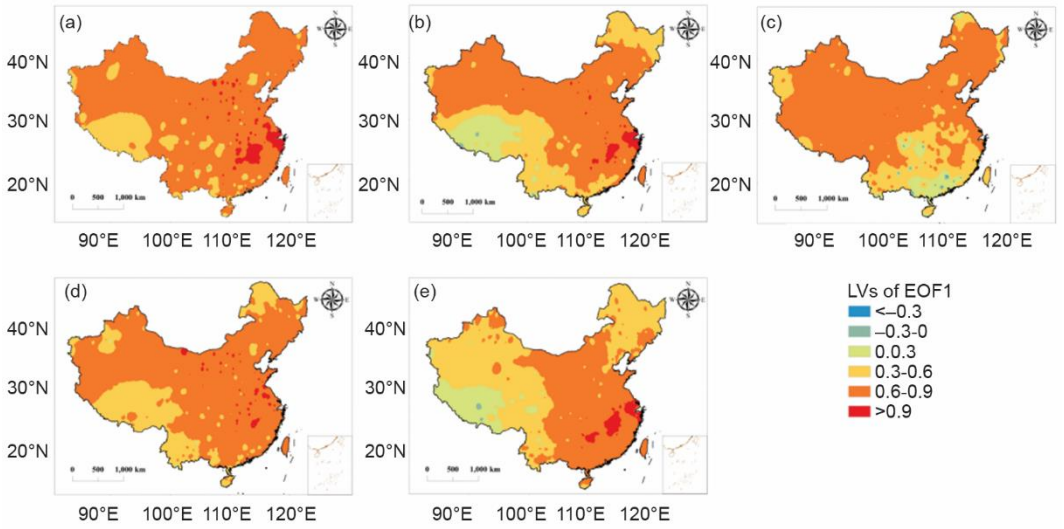

Figure 3. Spatial patterns of EOF1 of annual and seasonal CCI during 1966-2015 in China

The first spatial-temporal pattern of climate comfort variations

As shown in tab. 2, the explained variance of EOF1 of annual and seasonal CCI was more than 44%, which extracted most features of spatial variations in CCI. With almost all of the positive values in EOF1, the variation of climate comfort index followed the same trend in most regions of China. The loading value of 0.6 was used to distinguish the high correlated areas [23]. The regions with the high loading values (> 0.6) were observed in most regions except for the Tibet. The CCI in the Middle and lower Yangtze River was the most sensitive to climate change, as the loading values were more than 0.9. The sensitive areas were smaller in spring than those in autumn, though the spatial distribution of EOF1 was similar between spring and autumn. In contrast, the spatial distribution of sensitive areas in summer was greatly different from that in winter. As shown in fig. 3, the sensitive areas were mainly located in the central, eastern and southern China in winter, while they were observed in the northern and western China except for the southern and eastern China in summer.

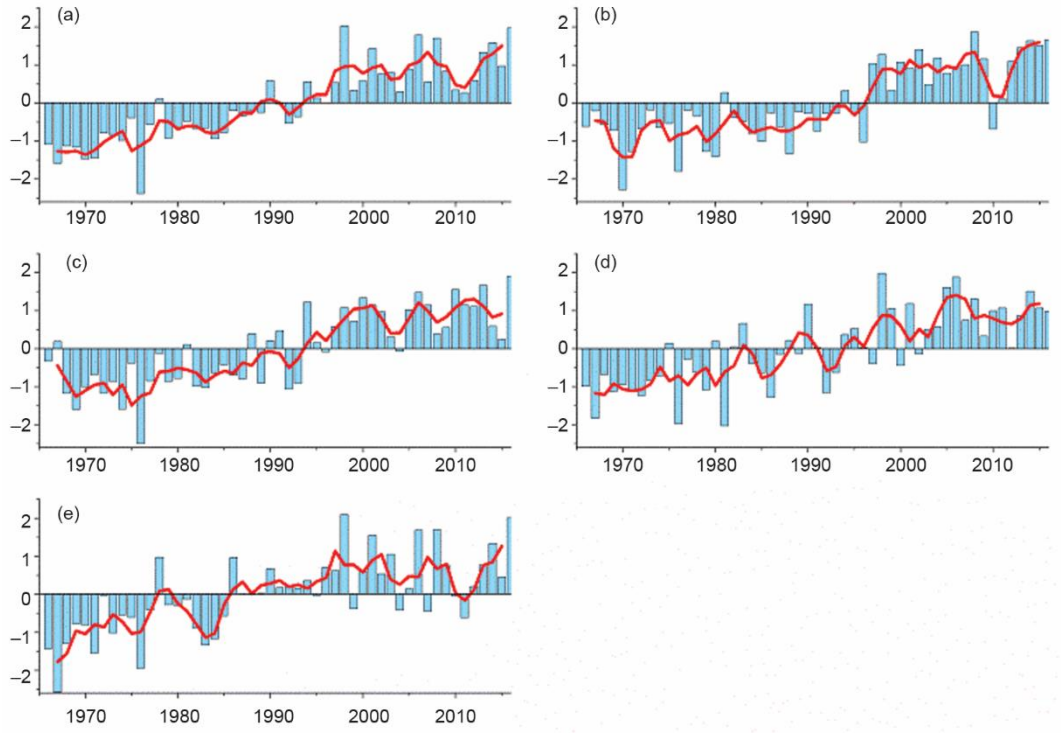

Figure 4. Temporal trends of PC1 of annual and seasonal CCI during 1966-2015 in China

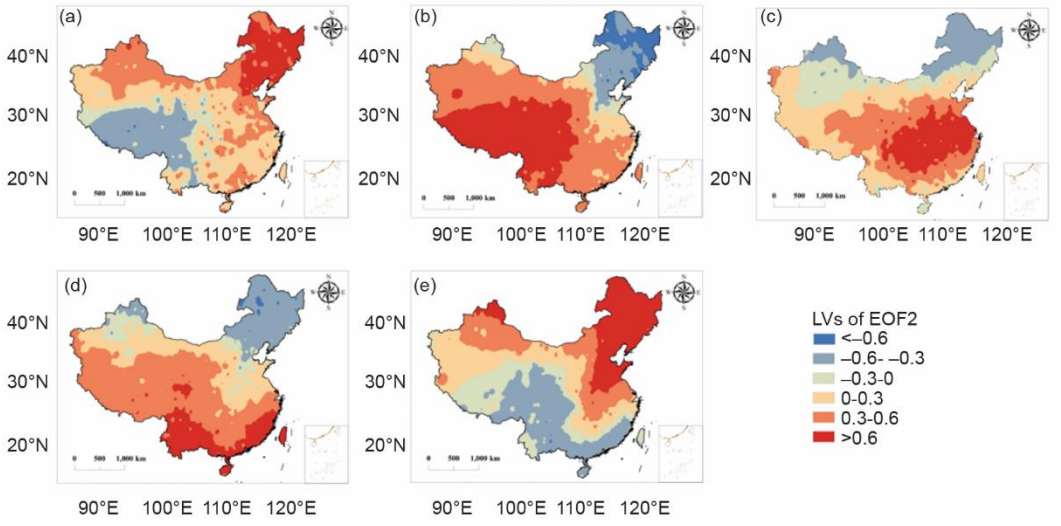

Figure 5. Spatial patterns of EOF2 of annual and seasonal CCI during 1966-2015 in China

The PC1 appeared significant upward trends from 1966 to 2016, which could be attributed to the obvious increasing trends in temperature and declining trends in wind speed. In consideration with the average values and their corresponding grades shown in fig. 4, it was notable that the climate in some regions would become more comfortable, while in some regions more uncomfortable. The climate in the northeastern and northwestern China was very uncomfortable, as the CCI values were between 25 and 38 and physiological sensation was very cold. The significant warming trends in these regions made the climate more comfortable to people. The increasing trends of CCI in the southern China in summer made the climate become hotter and people would feel more uncomfortable. In winter, CCI values decreased in the northwestern China (*i. e.* Tibet) with negative values of EOF1, which suggested that the climate in Tibet might become more cold and uncomfortable to people.

The second spatial-temporal patterns of climate comfort variations

The EOF2 displayed significantly asymmetric pattern. For annual CCI shown in fig. 6(a), the EOF2 values appeared negative in the southwestern China (*i. e.* Tibet Plateau), while they were positive in other parts of China. The regions with positive values accounted for more than 2/3 of China. The most significant variations were observed in the northeastern China, where the EOF2 values were larger than 0.6. The distribution of sensitive areas differed greatly between seasons. In spring, EOF2 values ranged from –0.67 to 0.78. The most sensitive areas with high loading values (*i. e.* > 0.6 or < –0.6) were mainly located in the southwestern and northern China. In contrast, the sensitive areas in EOF1 were observed in other regions. The sensitive areas were located in the central China in summer, the southwestern and southern China in autumn (*i. e.* Yunnan Province), and the northern China in winter, fig. 5.

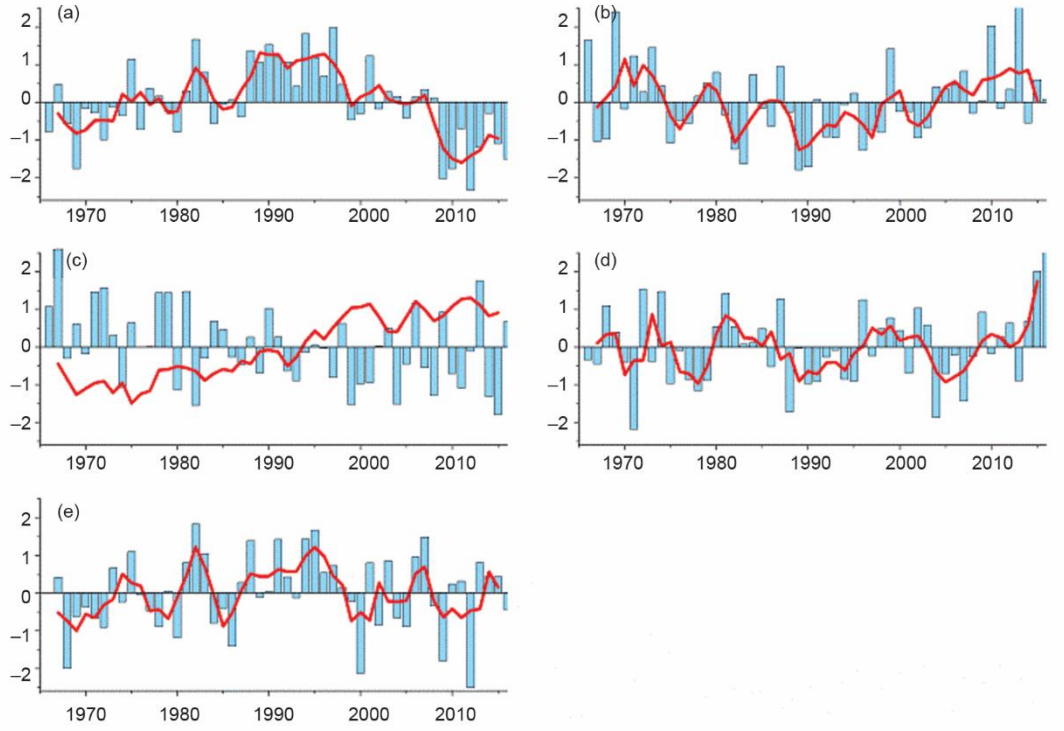

Figure 6. Temporal trends of PC2 annual and seasonal CCI during 1966-2015 in China

The PC2 represented the temporal trends in the positive regions. The regions with positive values of EOF2 displayed a contrary variation trend compared with those with negative values of EOF2. As shown in fig. 6, an obvious fluctuation between upward and downward trends was observed from 1966 to 2016. The main differences were the number of turning points. As shown in fig. 6(a), it was clear that the annual CCI values decreased between 1965 and 1990 and increased during 1995 and 2016 for the regions with positive EOF2 values (*i. e.* northern China). In contrast, the annual CCI exhibited the opposite trends for the regions with negative EOF2 values (*i. e.* Tibet). It suggested that annual CCI in the northern China experienced an increasing-decreasing trend, though an overall increasing trend was found over China.

Conclusion

The spatial pattern and its variability of climate comfort index in China during 1966-2016 were analyzed using the EOF analysis. The following conclusions can be drawn: the annual and seasonal CCI values showed a latitudinal gradient, and they generally increased towards the south except for the Qinghai-Tibet Plateau. In the first mode, the consistent increasing trend was a distinct feature in most regions of China. Featured with the high loading values (> 0.9), the annual CCI was the most sensitive to climate change in the Middle and lower Yangtze River. For seasonal CCI, the sensitive areas were observed in the central, eastern and southern China in winter, while in the northern and western China in summer. In the second mode, the inverse variation trends were detected between the regions with positive loading values and the regions with negative loading values. The PC2 represented the fluctuations between upward and downward trends. The annual CCI in the northeastern China experienced a decreasing-increasing trend, though the overall increasing trend was observed across China, its mechanism can be explained by the two-scale thermodynamics [24], which will be done in a forthcoming paper.

Acknowledgment

This work was supported by the National Key Research and Development Program of China (No. 2017YFC0506603, 2016YFC0401305), the State Key Program of National Natural Science of China (No. 41530635), and the General Program of National Natural Science Foundation of China (No.51679007, 51379013).

References

[1] Freitas, C. R., *et al.*, A Comprehensive Catalogue and Classification of Human Thermal Climate Indices, *International Journal of Biometeorology*, *59* (2015), 1, pp. 109-120
[2] Brunt, D., Climate and Human Comfort, *Nature, 155* (1945), May, pp. 559-564
[3] Zare, S., *et al*, Comparing Universal Thermal Climate Index (UTCI) with selected thermal indices/environmental parameters during 12 months of the year, *Weather Climate Extreme, 19* (2018), Mar., pp. 49-57
[4] Cheung, P. K., *et al*, Improved Assessment of Outdoor Thermal Comfort: 1-Hour Acceptable Temperature Range, *Building and Environment, 151* (2017), Mar., pp. 303-317
[5] Shakoor, A., *et al.*, Effects of Climate Change Process on Comfort Climate in Shiraz Station, *Journal of Environmental Health Science and Engineering, 5* (2008), 4, pp. 269-276
[6] Mochida, A., *et al*, Prediction of Wind Environment and Thermal Comfort at Pedestrian Level in Urban Area, *Journal of Wind Engineering and Industrial Aerodynamics, 96* (2008), 10-11, pp. 1498-1527
[7] Xu, Y. Q., *et al.*, Study on Differences of Temperature and Humidity and Vertical Distribution of Human Comfort between City and Countryside of Heilongjiang Province in Summer, *Meteorological and Environmental Research, 5* (2014), 2, pp. 41-44

[8] Xiong, J., *et al*, Effects of Temperature Steps on Human Health and Thermal Comfort, *Building and Environment, 94* (2015), Dec., pp. 144-154
[9] Buddhi, P., *et al.*, The Influence of Wind Speed on New Particle Formation Events in an Urban Environment, *Atmospheric Research, 215* (2018), Jan., pp. 37-41
[10] Terjun, W. H., Physiologic Climates of the Contentious United States: Bio Climatic Classification Based on Man, *Annals of the Association of American Geographers, 5* (1996), 1, pp. 141-179
[11] Wang, C. Z., *et al.*, Nonlinear Relationship between Extreme Temperature and Mortality in Different Temperature Zones: a Systematic Study of 122 Communities Across the Mainland of China, *Science of the Total Environment, 586* (2017), May, pp. 96-106
[12] Ibrahim, H. M., *et al.*, Spatio-Temporal Patterns of Soil Water Storage under Dryland Agriculture at the Watershed Scale, *Journal of Hydrology, 404* (2011), 3-4, pp. 186-97
[13] Li, Q., *et al.*, A Global Weighted Mean Temperature Model Based on Empirical Orthogonal Function Analysis, Advances in Space Research, *61* (2018), 6, pp. 1398-1411
[14] Richman, M. B., *et al.*, Relationship between the Definition of the Hyperplane width to the Fidelity of Principal Component Loading Patterns, *Journal of Climate, 12* (1999), 6, pp. 1557-1576
[15] Wypych, A., *et al.*, Spatial and Temporal Variability of the Frost-Free Season in Central Europe and its Circulation Background, *International Journal of Climatology*, *37* (2017), 8, pp. 3340-3352
[16] Wu, F. F., *et al.*, Regional and Seasonal Variations of Outdoor Thermal Comfort in China from 1966 to 2016, *Science of the Total Environment, 665* (2019), May, pp. 1003-1016
[17] Oh, J., *et al.*, Real-Time Forecasting of Wave Heights Using EOF-Wavelet-Neural Network Hybrid Model, *Ocean Engineering, 150* (2018), Feb., pp. 48-59
[18] Yang, X. H., *et al.*, Chaos Gray-Coded Genetic Algorithm and its Application for Pollution Source Identifications in Convection-Diffusion Equation, *Communications in Nonlinear Science and Numerical Simulation*, *13* (2008), 8, pp. 1676-1688
[19] Jolliffe, I. T., *Principal Component Analysis*, 2nd ed., Springer, New York, USA, 2002, pp. 149
[20] Hannachi, A., A Primer for EOF Analysis of Climate Data. Department of Meteorology, Ph. D. thesis, University of Reading, Reading, UK, 2004, pp. 133
[21] Piairo, H., *et al.*, Spatial Modeling of Factor Analysis Scores, *Environmental Science & Pollution Research International, 21* (2014), 23, pp. 13420-13433
[22] Schreck III, C. J., *et al.*, Variability of the recent climate of Eastern Africa, *International Journal of Climatology, 24* (2004), 6, pp. 681-701
[23] Cheng, L. J., *et al.*, Regionalization Based on Spatial and Seasonal Variation in Ground-Level Ozone Concentrations Across China, *Journal of Environmental Sciences, 67* (2018), 5, pp. 179-190
[24] He, J. H., Ji, F. Y., Two-Scale Mathematics and Fractional Calculus for Thermodynamics, Thermal Science, *23* (2019), 4, pp. 2131-2133

Paper submitted: April 30, 2019
Paper revised: August 1, 2019
Paper accepted: August 8, 2019